Rev. FCA UNCUYO. 2018. 50(2): 33-47. ISSN impreso 0370-4661. ISSN (en línea) 1853-8665.

The phenomenon of cavitation in grapevine... Unravelling implicated mechanisms

El fenómeno de la cavitación en vid... Descifrando los mecanismos implicados

Inés Hugalde [1], Marcos Bonada [2], Hernán Vila [1]

Originales: *Recepción:* 18/04/2017 - *Aceptación:* 07/11/2017

Abstract

Cavitation is a physiological dysfunction that takes place in the xylem of water stressed plants leading to a loss of hydraulic conductance (k_L) as the vessels are filled with air. This impacts water supply, water potential (Ψ_L) and canopy hydration. Stomatal clossure is an effective response upon diminishing momentary or seasonal foliar hydraulic contents. Depending on each plant, stomata may close preventing catastrophic cavitations. This research intended to understand how stomatal control acts upon cavitation events in two contrasting grapevine varieties, Syrah and Grenache. A mechanistic model was developed based on the water and vapour fluxes, k_L, stomatal conductance (g_s), and vulnerability to cavitation. The theoretical model explains plant drough responses and catastrophic cavitation avoidance. Water stressed grapevines couple g_s with k_L in order to avoid embolism. It is not stomatal closure, by istself, the controlling mechanism. Grapevines under mild water stress, do not need to completely close their stomata in order to avoid cavitation, therefore, photosynthesis is not completely impeded, and the cost in terms of carbon assimilation is less than expected for other species.

Keywords
cavitation • stomatal conductance • hydraulic conductance • mechanistic model • Syrah • Grenache

1 INTA (Instituto Nacional de Tecnología Agropecuaria) EEA Mendoza. San Martín 3853. Luján de Cuyo, Mendoza. Argentina. hugalde.ines@inta.gob.ar
2 South Australian Research and Development Institute. Waite Campus. Adelaide. SA 5064. Australia.

Resumen

La cavitación es una disfunción fisiológica que ocurre en el xilema de las plantas bajo déficit hídrico, y que entraña una pérdida de su conductancia hidráulica (k_L), cuando algunos vasos se llenan de aire. Esto incide negativamente sobre la oferta de agua y afecta el potencial hídrico foliar (Ψ_L) y la hidratación de la canopia. El cierre estomático es una respuesta efectiva ante la disminución del contenido hídrico. Dependiendo de la especie vegetal, los estomas suelen cerrase para evitar la cavitación catastrófica. Mediante un modelo mecanístico, que se construyó teniendo en cuenta los flujos de agua y vapor, las k_L y conductancia estomática (g_s), y la vulnerabilidad del xilema a cavitar; se probó que g_s no es la única variable responsable de frenar la embolia. Se determinó que g_s y k_L están íntimamente asociadas y que este acople entre ambas conductancias es lo que frena la embolia. Se concluyó que, en la vid y bajo niveles de estrés hídrico moderado, no es necesario un cierre estomático para controlar la cavitación. Por esto, el mecanismo de control de la cavitación en la vid no conlleva un costo en términos de intercambio gaseoso.

Palabras clave
cavitación • conductancia estomática • conductancia hidráulica • modelo mecanístico • Syrah • Grenache

Introduction

Drought resistant crops have adaptive physiological and morphological traits that allow them to survive and grow under severe water deficit, resisting dehydration (14, 24). The origin of plant dehydration is embolism and catastrophic cavitation. In a dry soil, with low water potential, increasing xylem tension triggers cavitation. This phenomenon consists on the formation of air bubbles inside the xylem vessels, and subsequently, water column breakage (35). As consequence, the plant suffers a loss of hydraulic conductance (k_L) and desiccation (6, 11, 34, 35). Vulnerability curves relate percentage loss of conductivity (PLC) or embolism to increasing applied positive pressures causing that drop of k_L. This pressure may be paralleled to the xylem tension, given that it can be considered equal (in absolute value), but opposite, to the negative pressure inside the xylem (1, 12, 31, 34).

It is well known that stomatal control prevents excessive water loss in an attempt to maintain k_L and prevent desiccation under high evaporative demand. Several authors have also concluded that stomatal modulation limits cavitation (4, 8, 15, 19, 21, 28) and that the mechanism is subjected to hydraulic and hydromechanic laws (3, 4, 11). In general, grapevines have been considered a drought avoiding species due to an efficient stomatal control (8). Most of the water that enters the plant (constituting k_L), leaves through opened stomata (depending on stomatal conductance, g_s) as transpiration (E) (9).

In this sense, many authors have already studied the relationship between g_s and k_L, concluding that in most species, including grapevine, both conductances are tightly correlated (17, 18, 21, 29, 39). While aquaporins, in roots, act as entrance valves for water (20, 28), stomata in

leaves act as water vapour exit valves that limit transpiration (E).

However, recent insights cast doubt on the main role of stomatal closure on the embolism-avoidance strategy (38, 39), besides the fact that the actual mechanism is still not elucidated (2, 16). In addition, grapevines have shown to own a highly resistant xylem (10) that cavitates at higher tensions than previously thought, keeping k_L between certain values before stomata respond. In this context, this research intended to study the cavitation phenomenon in grapevines and the control mechanisms involved. It tried to comprehend on a mechanistic manner, the stomatal functioning, its relation to the cavitation phenomenon, and the physical laws that rule them. This was achieved by complementing the construction of a functional and dynamic model with the comparison of two contrasting varieties, Syrah and Grenache, under two different water treatments, grown in pots, inside a greenhouse. These varieties have been reported as opposite with regards to stomatal behaviour, isohydric and anisohydric, respectively (8, 9), However, this classification is currently under strong debate (8, 14, 19, 21, 29). Given this controversy, this study tested the model as well as varieties' behaviour under these conditions.

Model development

Several models describe stomatal functioning (8). The present model includes several sub-models and relates them in an attempt to explain embolism control by hydraulic traits in grapevine, adding the "vulnerability to cavitation element", and clarifying the coupling mechanism that achieves embolism control.

The model is based on the Ohm's law analogue concept (37) stating that the flow (J_w) escaping through stomata, called transpiration (E), constitutes the driving force that moves water along the xylem vessels. This suction inside the xylem vessels is expressed in terms of water potential (Ψ; MPa). Finally, this Ψ difference between soil and leaves (ΔΨ) allows water to move from one place to the other (13, 37).

$$J_w = \frac{\Delta\Psi}{R} = k_L . \Delta\Psi = E; \qquad (1)$$

$$\Delta\Psi = \Psi_{soil} - \Psi_L \qquad (2)$$

where:

J_w = E, is transpiration (mmol H_2O m^{-2} s^{-1})

R = hydraulic resistance = $1/k_H$ (1/ (mmol H_2O m^{-2} s^{-1} MPa^{-1}))

k_L = hydraulic conductance (mmol H_2O m^{-2} s^{-1} MPa^{-1})

ΔΨ = water potential difference (MPa)

Ψ_{soil} = soil water potential (MPa)

Ψ_L = leaf water potential (MPa)

Assuming that species like grapevines have null capacitance (25); (meaning that there is no water storage due to the water potential difference), J_w equals E (1), and may be expressed by Fick´s law as follows:

$$E = \frac{(e_{sT(L)} - e_a)}{P_a . (gs^{-1} + gb^{-1})} \qquad (3)$$

where:

E = transpiration (mmol H_2O m^{-2} s^{-1})

$(e_{sT(L)} - e_a)/Pa" = q´$ is the difference of water vapour concentration between leaf and atmosphere, the vapour pressure gradient from leaf to air (dimensionless variable).

$(g_s^{-1} + g_b^{-1})$ = sum of stomatal and boundary layer resistances (1/mmol H_2O m^{-2} s^{-1}).

Then, by replacing (2) and (3) in (1), we obtained (4)

$$\Psi_L = \Psi_{soil} - \frac{q'/g_s^{-1} + g_s^{-1}}{k_L} \qquad (4)$$

where:
q' = leaf to air vapour pressure gradient.

Eq. (4) formalizes the relationship between Ψ_L, q' g_s and k_L.

The next step was to relate plant embolism (Emb) to the hydraulics described. Emb inversely depends on water potential (Ψ). For more negative values of Ψ, higher percentages of Emb can be measured. In the model, Emb was interpreted by fitting the sigmoid vulnerability curves to a piece-wise defined function, shown as follows in figure 1.

In the first piece of the function, up to certain $\Psi_L = \Psi_{L1}$, Emb equals cero (5). This part of the function is called "lag" and corresponds to a Ψ_L range where no embolism takes place. When Ψ_L diminishes because of increasing water deficit, exceeding Ψ_{L1}, Emb lineally depends on Ψ_L, and grows until maximum Emb -*i.e.* 100%- is achieved for $\Psi_L = \Psi_{L2}$ (6). On or after Ψ_{L2}, Emb equals 1 (or 100%; (7); figure 1).

$$\begin{cases} Emb = 0 & ; \quad \Psi_L \leq \qquad (5) \\ Emb = a + b.\Psi_L ; \Psi_{L1} \geq \Psi_L \leq \Psi_{L2} & (6) \\ Emb = 1 & ; \quad \Psi_L \leq \Psi_{L2} \qquad (7) \end{cases}$$

By trigonometry, equation (6) can mathematically be expressed as (8):

$$Emb = \frac{\Psi_L - \Psi_{L1}}{\Psi_{L2} - \Psi_{L1}} ; \Psi_{L1} \leq \Psi_L \leq \Psi_{L2} \quad (8)$$

Then, by replacing (4) in (6) the suffered Emb, (Equation 9) is obtained as output of the model for the part of the function in which Emb linearly depends on Ψ_L.

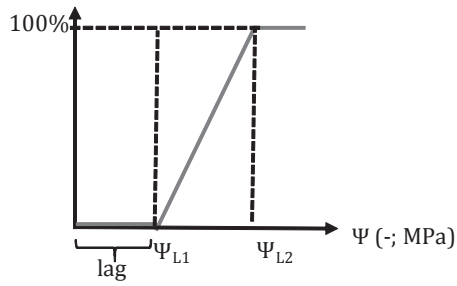

"Lag" indicates the pressures under Ψ_{L1} where no embolism takes place. Note that Ψ are negative values.

El "lag" indica la presión bajo la cual no existe embolia. Los valores de Ψ son negativos.

Figure 1: Theoretical vulnerability curve for grapevines. Ψ_{L1}, the pressure at which embolism starts, and Ψ_{L2}, the pressure at which embolism reaches 100%.

Figura 1: Curva teórica de vulnerabilidad para vid. Ψ_{L1}, la presión a la cual comienza la embolia, y Ψ_{L2}, la presión a la cual existe embolia máxima.

$$Emb = \frac{(\Psi_{soil} - \frac{q/g_s^{-1} + g_b^{-1}}{k_L}) - \Psi_{L1}}{\Psi_{L2} - \Psi_{L1}} \qquad (9)$$

Equation 9 probes that plant embolism effectively depends on g_s, although not in a straightforward manner, but through its interaction with other variables, like q' (that depends on leaf temperature T_L and atmospheric variables), the boundary layer conductance (g_b, that varies with wind speed) and most importantly, with k_L, that depends on root aquaporin activity (36). With respect to g_s *vs.* k_L, daylong correlation has been widely proven and corroborated by this study ($R = 0.8438$, $p = 0.000$, figure 2, page 37).

This study also created Δg_s, a new variable representing the g_S *vs.* k_L ratio.

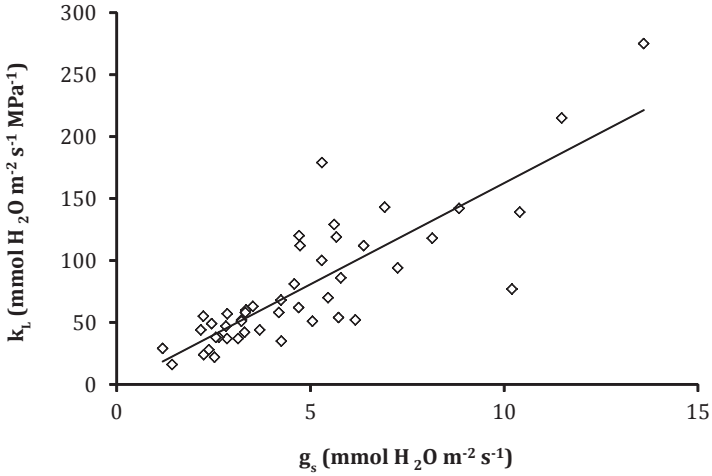

Values are individual measuremets. / Los puntos son valores individuales de medición.

Figure 2. Correlation between stomatal conductance (g_s, mmol H_2O m^{-2} s^{-1}) and hydraulic conductance (k_L, mmol H_2O m^{-2} s^{-1} MPa^{-1}) for Syrah.

Figura 2. Correlación entre conductancia estomática (g_s, mmol H_2O m^{-2} s^{-1}) y conductancia hidráulica (k_L, mmol H_2O m^{-2} s^{-1} MPa^{-1}) para Syrah.

The model also shows the feedback loop between Emb and k_L, stating that Emb depends on k_L, while, at the same time, k_L depends on Emb, as the former diminishes when the last rises.

Figure 3 (page 38), shows the dynamic mechanistic model that explains how the relationship between g_s and k_L controls embolism, and how embolism, in turn, modifies k_L in a feedback loop. The k_L (2) is the result of a k_L before embolism (k_{Lbe} or maximum k_L, 3), then affected by embolism (1) and dependent on daytime and Ψ_{soil}.

The model adopted several already existing models to fit into the general model. The g_s (5) is interpreted by the Buckley *et al.* model (2003); g_b and leaf temperature (T_L) are expressed by the Campbell and Norman (2012) equations (4); $\Psi_{\pi g}$ (osmotic water potential of the guard cell), included in g_s (5), is empirically expressed by Taiz and Zeiger (1998) and Tardieu and Simonneau (1998). Input variables are Ψ_{L1}, Ψ_{L2}, daytime (hour), Ψ_{soil}, T_a, e_a/P_a, wind speed and solar radiation. The model output is Embolism (1).

Model parameterizing

To parameterize the model, an experiment with Grenache and Syrah plants was conducted under field capacity and water sstress. Gas exchange and Ψ_L were measured during a complete day, from predawn to 18 h. The k_L was calculated for each moment along the day, and a time dependent equation was then fitted to the data. Vulnerability curves were constructed and embolism achieved along the day was estimated.

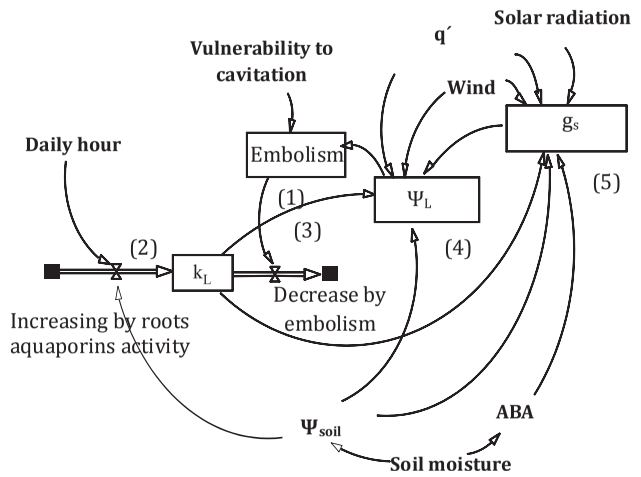

ψ_{L1}, ψ_{L2}, time(hour), ψ_{soil}, Ta,q',wind,solar radition; entry variables

$$\begin{cases} Emb = 0 & ; \quad \Psi_L \leq \\ Emb = a + b.\Psi_L & ; \Psi_{L1} \geq \Psi_L \leq \Psi_{L2} \\ Emb = 1 & ; \quad \Psi_L \leq \Psi_{L2} \end{cases} \quad (1)$$

$$k_L = k_{Lbe}(1 - \mathrm{Emb}) \quad (2)$$

$$k_{Lbe} = \mathrm{f}(\mathrm{time}, \Psi_{soil}) \quad (3)$$

be denotes *before* embolism, Empiric; Vandeleur *et al.* (2009)

$$\Psi_L = \Psi_{soil} - \frac{q'/g_s^{-1} + g_b^{-1}}{k_L} \quad \text{Van del Honert (1948)} \quad (4)$$

$$g_b = 1.4 \cdot 0.147\sqrt{\mu/0.8.w_L} \quad \text{Campbell and Norman (2012)}$$

$$q' = (es(TL) - ea)/Pa \quad \text{Taiz and Zieger (1998)}$$

$$\Psi_{\pi g} = f(solarradition, [ABA]) \quad \text{Tardieu and Simmoneau (1998)}$$

$$g_s = \frac{x.(-\Psi_{\pi g} + \Psi_{\pi e} - M \cdot \Psi_{soil} + M\Psi_{\pi g}}{1 - X \cdot (\mathrm{M} \cdot k_L^{-1} - f_g \cdot r_g \cdot \frac{D_b}{P}} \quad \text{Buckley } \textit{et al.} \text{ (2005)} \quad (5)$$

Equations on the right are represented by numbers in the figure. The environmental mechanics are formalized by the Campbell and Norman (1998) equations of boundary layer conductance (g_b) and atmospheric deficit (q') then included in the Buckley *et al.* (2005) equation for stomatal conductance (g_s) (5). The Van den Honert (1948) equation (4) establishes leaf water potential (Ψ_L) that later will define plant hydraulic conductance (k_l). Hydraulic conductance before embolism (k_{be}) formalizes the relationship between maximum k_L and k_L after embolism being the formmer subjected to soil water potential and daytime, according to Vandeleur *et al.* (2009), (2) and (3). Finally, the equations expressing Embolism are shown in (1). Equation (1) defines Xylem Embolism based on the parameters that characterize the vulnerability curve of a definite species. Note that this model is constructed based on several mechanistic models, and all of them joined together in one bigger mechanistic model via the Embolism functional equation.

Las ecuaciones de la derecha se representan por números en el diagrama. Los mecanismos ambientales se formalizan mediante las ecuaciones de Campbell y Norman (1998) para la conductancia de la capa límite (g_b) y el déficit atmosférico (q') que luego se incluyen en la ecuación de Buckley *et al.* (2005) para conductancia estomática (g_s) (5). La ecuación de Van den Honert (1948) (4) define el potencial hídrico foliar (Ψ_L) que luego definirá la conductancia hidráulica (k_L). La ecuación de conductancia hidráulica antes de la embolia (k_{be}) formaliza la relación entre la k_L máxima y la k_L después de la embolia. La primera depende del potencial hídrico del suelo (Ψ_{soil}) y el momento del día, según Vandeleur *et al.* (2009), (2) and (3). Finalmente, las ecuaciones que expresan el curso de la *Embolia* se muestran en (1). La ecuación (1) define *Xylem Embolism* basándose en los parámetros que caracterizan la curva de vulnerabilidad de una especie definida. Nótese que este modelo integra modelos mecanísticos previos en uno solo, mediante la ecuación de embolia de la vid.

Figure 3. Mechanistic dynamic model formulated to explain how embolism control takes place by stomatal and hydraulic coupling.

Figura 3. El modelo dinámico se construyó para explicar cómo la embolia es controlada por el acople entre la conductancia estomática e hidráulica.

Materials and methods

Vines and site

The experiment was conducted during the 2012/2013 season at INTA Experimental Station, in Mendoza, Argentina.

A factorial desing combining 2-years-old Syrah and Grenache grapevines and two water regimes was established on December of 2012. In quadruplicate, dormant own-rooted vines were removed from their 4-L pots and replanted on a sandy loam substrate in 15-L pots.

Water regimes, namely field capacity (FC) and water deficit (WD), were irrigated with 100% and 50% of the fraction of transpirable soil water (FTSW), respectively, as follows: Immediately after replanting all vines were irrigated to saturation and water treatments were applied. The FC treatment was watered every two days keeping 100% FTSW whereas the WD treatment was left without irrigation for a week until it reached the targeted soil moisture of 50% FTSW (0.16 g/g). After WD pots achieved the desired soil moisture, pots were watered every two days replenishing the transpired water. Water regimes were maintained for three months. Moisture was measured every two days using moisture probes (ECH2O EC-5 sensors, Decagon devices, USA). Vines were trained to one shoot and grown in a greenhouse with daily average temperature of 25°C and photosynthetic active radiation of 800 μmoles $m^{-2} \bullet s^{-1}$.

Water potential and gas exchange measurements

After 3 months, a portable photosynthesis system (CIRAS-2, PP Systems, Hertfordshire U.K) was used to measure instantaneous leaf gas exchange. Measurements were carried out every two hours from 6am to 6pm.

The CO_2 concentration of the incoming air was kept at 375 μmol•mol^{-1}. The same leaves used for gas exchange assessment were used to measure leaf water potential (Ψ_L), with a Scholander pressure chamber (Biocontrol, Córdoba, Argentina), according to Hsiao (37). Predawn water potential (Ψ_{PD}) was considered as proxy to soil water potential (Ψ_{soil}).

Water vapour concentration at leaf temperature ($e_{sT(L)}$/Pa; hPa), was calculated via the Teten equation.

$$e_{sT(L)} = 6.11 \times Exp\left(\frac{17.502 \times T_L}{T_L + 240.97}\right) \quad (10)$$

where:

T_L = leaf temperature

The k_L was calculated through the Van den Honert equation, with Ψ_{soil}, Ψ_L, and E for every assessed moment of the day.

Daylong leaf embolism (Emb) was estimated from the daily Ψ_L course and vulnerability curves, for each plant. Both curves were related and the positive pressures achieved for the vulnerability curves were directly linked to the Ψ_L measured along the day, assigning an embolism value to each moment and plant.

Vulnerability curves

The loss of k_H to increasing Ψ_L, *i.e.* cavitation, was studied by constructing vulnerability curves for each plant: after water potential and gas exchange measurements, shoots were harvested and transported to the laboratory. Previously, every leaf was removed from the stem, and cut surfaces were sealed with contact glue. Vulnerability curves were constructed following the "Air Injection Long" method (10), using a

double ended pressure sleeve connected to a Scholander pressure chamber (Biocontrol, Córdoba, Argentina;). First, the shoots were flushed for 30 minutes using distilled, degassed 5% potassium hypochlorite (KClO) solution, removing all embolisms and obtaining maximum k_H (k_{Hmax}). Then, successive pressure cycles were imposed. The air pressure in the chamber was increased to a specific value and held for 10 minutes before it was reduced back to cero. Air pressure was successively increased to higher levels as hydraulic measures were taken, obtaining k_H for each cycle. Percentage loss of conductivity (PLC) was calculated for each cycle relative to k_{Hmax}.

$$PLC = 100 \times (1-(k_i / k_{max})) = (k_{max} - k_i) / k_{max.}$$

Statistics and data analysis

Differences between treatments were assessed by multifactor and one-way ANOVA, followed by LSD test ($p < 0.05$) using Stat Graphics Plus (Statistical Graphics Corp.; StatSoft, Inc., 2003). When ANOVA assumptions were not met, non-parametrical analyses were carried out.

Results

Water relations: water potential and stomatal conductance

The imposed water deficit had an evident effect on Ψ_L. Water deficit (WD) treatments provoked a significantly lower (more negative) Ψ_L than field capacity (FC). For midday water potential (Ψ_{md}), treatment interaction was significant (varieties *vs.* water treatments; $p = 0.0333$). As for g_s, WD treatments had significantly lower values than FC, during the whole day ($p = 0,01$; figure 4, page 41).

Once all vulnerability curves were obtained, piece-wise defined functions were fitted as described in the "Model development" section: The first piece of the function, were no cavitation or embolism (Emb) has already happened, is called "lag" and equals cero for Emb; while the second part of the function, showing increasing cavitation, is fitted to a straight line equation (figure 1, page 36 and figure 5, page 41).

The ANOVA analysis for the straight line fitting parameters *a* (intercept) and *b* (slope) showed that neither statistically significant interaction, nor significant differences existed among varieties or water treatments (table 1, page 42). This means that under this experimental conditions, no xylem adaptation upon water stress occurred.

Xylem embolism *vs.* water relations, throughout day

Estimated embolism throughout the day was only achieved in four cases, as most plants had vulnerability curves with long lags starting from -1.5 MPa, while this Ψ_L value was generally not achieved in the greenhouse. As leaf embolism directly depends on Ψ_L, both variables followed similar, though opposite daily courses. Lower Ψ_L corresponded to higher cavitation values (figure 6, page 42).

When daily courses of embolism and g_s were observed for the four plants that did cavitate, no relation between both variables could explain embolism control. Stomatal closure events (reduction on g_s) *vs.* embolism detention did not correlate throughout the day, meaning that g_s, *per se*, is independent of embolism (figure 7 page 42). This conclusion was already achieved theoretically by means of the model that clearly showed that the controlling switch was, in fact, a coupling event between g_s and k_L, (and not g_s itself) .

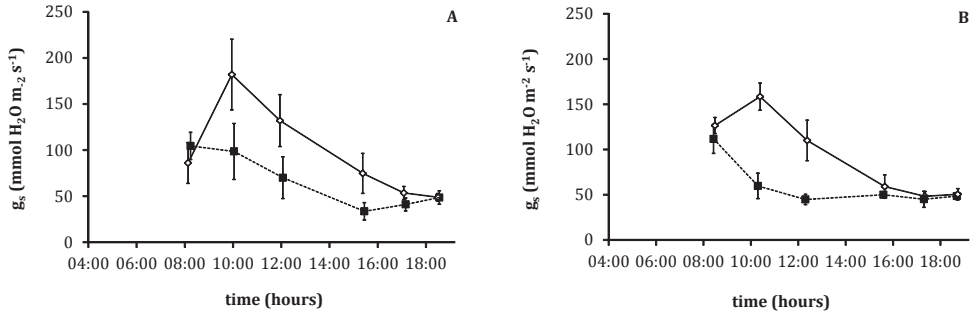

Each point corresponds to the mean ± one SE for water deficit (WD; dotted line) and field capacity (FC; solid line) treatments.

Cada punto corresponde a la media ± un error para déficit hídrico (WD; línea de puntos) y capacidad de campo (FC; línea entera).

Figure 4. Daily course of stomatal conductance (g_s, mmol H_2O m^{-2} s^{-1}) for Grenache (A) and Syrah (B).

Figura 4. Dinámica de la conductancia estomática a lo largo de un día (g_s, mmol H_2O m^{-2} s^{-1}) para Grenache (A) y Syrah (B).

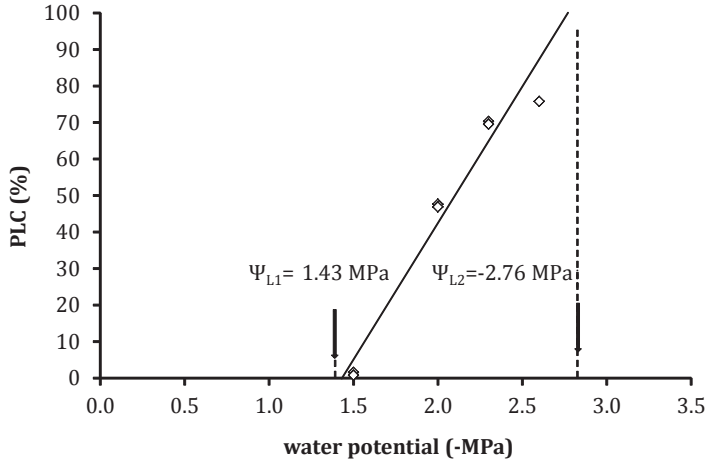

Dots indicate values from a single shoot. Straight line indicates linear fitting.

Los puntos indican los valores medidos en un tallo. La línea indica el ajuste lineal obtenido.

Figure 5. Vulnerability curve measured in Grenache under water stress [percentage loss of hydraulic conductance (PLC) *vs.* pressure (ΨL)]. The pointed Ψ_{L1} and Ψ_{L2} are the pressures at which xylem embolism starts and equals 100%, respectively. Under Ψ_{L1} no embolism takes place.

Figura 5. Curva de vulnerabilidad medida en Grenache bajo estrés hídrico [porcentaje de pérdida de conductancia hidráulica (PLC) *vs.* presión (Ψ_L)]. Los valores de Ψ_{L1} y Ψ_{L2} señalados son las presiones a las que la embolia comenzó y alcanzó el 100%, respectivamente. Debajo de Ψ_{L1} no existe embolia.

Table 1. Straight line fitting parameters b (slope) and a (intercept) for vulnerability curves in Grenache and Syrah cultivars, under field capacity (FC) and water deficit (WD). Data are means values.

Tabla 1. Parámetros de ajuste lineal b (pendiente) y a (intercepto) para curvas de vulnerabilidad en Grenache y Syrah, bajo capacidad de campo (FC) y déficit hídrico (WD). Los datos son medias de mediciones y los *p*-values provienen del ANOVA.

Variable	b	a
Cultivar (C)		
Grenache	-0.8855	-1.9221
Syrah	-0.8678	-1.4316
p value	0.9615	0.6209
Water treatment (W)		
FC	-0.6077	-1.0930
WD	-1.1457	-2.2607
p value	0.1596	0.2501
p value (C × W))	0.8775	0.9983

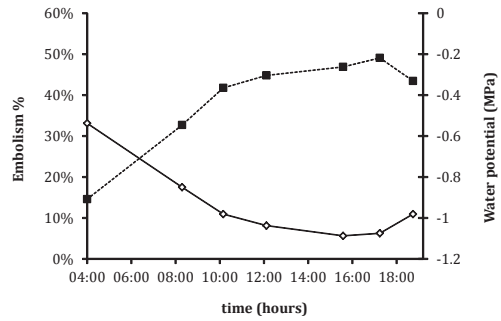

Figure 6. Daily course of water potential (Ψ_L; solid line) and embolism (dotted line). Values are means from the three Syrah vines and the one Grenache plant suffering embolisms throughout the day.

Figura 6. Dinámica del potencial hídrico (Ψ_L; línea entera) y la embolia (línea punteada) a lo largo del día. Los valores son la media para tres plantas de Syrah y una planta de Grenache en condiciones de embolia.

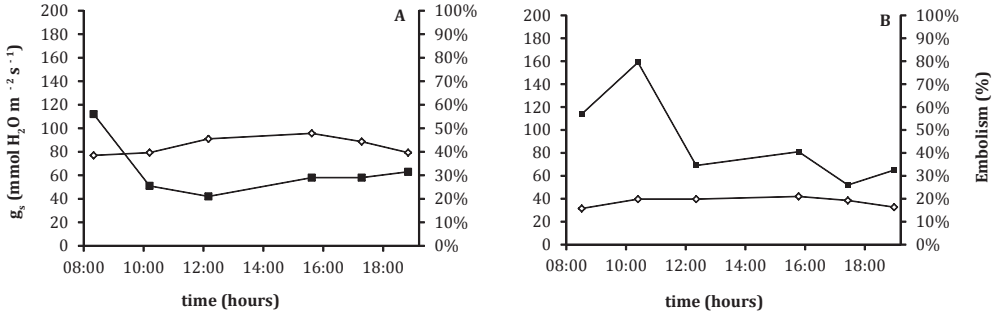

Figure 7. Daily course of stomatal conductance (g_s; black squares) and embolism (black diamonds) for two vines that suffered embolism under water deficit (A) and under field capacity (B). Clear independence between both curves is shown.

Figura 7. Cinética de la conductancia estomática (g_s; cuadros negros) y la embolia (diamantes blancos) a lo largo de un día para dos vides que sufren embolia bajo condiciones de estrès hidrico (A) y bajo capacidad de campo (B). Notar la clara independencia entre ambas curvas.

Simulations

Figure 8, shows how embolism, Ψ_L, g_s and k_L behaved under water stress (Ψ_{soil}=-0.2), constant environmental conditions and variable guard cell osmotic adjustment (π_g). The π_g modifies g_s, in a significant manner, (Buckley *et al.*, 2003). In this case, π_g was augmented by 20% for case A; and diminished by 20% in case B. Notice that as Ψ_L turns more negative and achieves -2 MPa, embolism starts and g_s couples with k_L (Δgs = 28), allowing a maximum embolism of 45% for simulation B. For simulation A, were Ψ_L does not grow over the threshold value and no embolism takes place, the coupling is much less evident (Δg_s = 16).

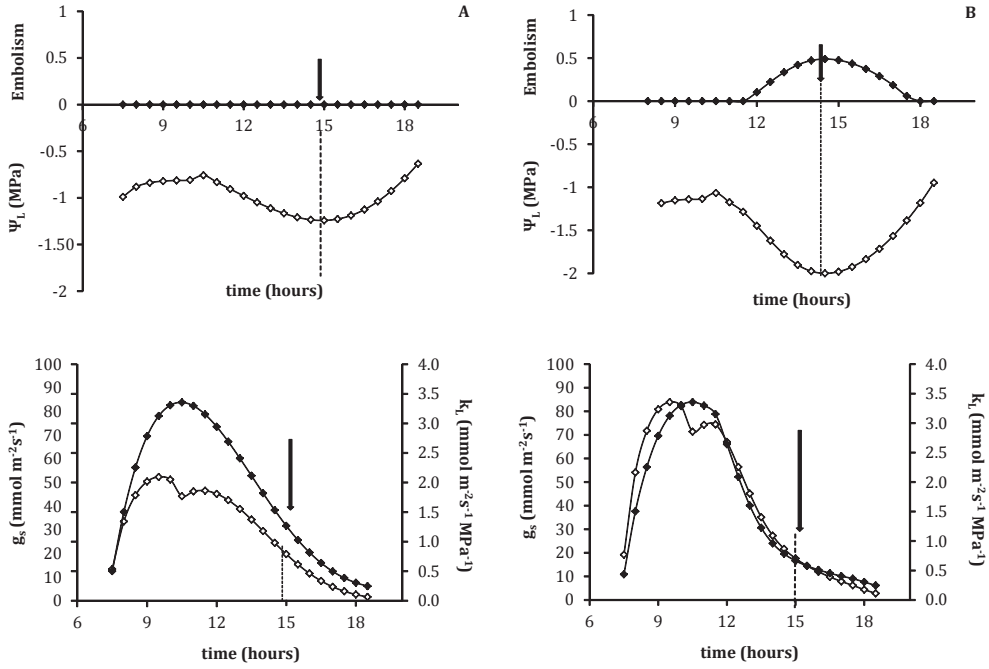

Arrows in figure A show that no embolism occurs, stomatal conductance (g_s) does not couple with hydraulic conductance (k_L) and Δg_s=16. Arrows in figure B show that as soon as embolism starts, stomatal conductance (g_s) couples with hydraulic conductance (k_L) achieving a Δg_s=28. (Embolism and k_L; black diamonds; Ψ_L and g_s; white diamonds).

Las flechas en la figura A muestran que la embolia no ocurre, la conductancia estomática (g_s) no se acopla con la conductancia hidráulica (k_L) y Δg_s=16. Las flechas en la figura B indican que en cuanto comienza a haber embolia, la g_s se acopla con la k_L alcanzando un Δg_s=28. (Embola y k_L; rombos negros; Ψ_L y g_s; rombos blancos).

Figure 8. Simulations of embolism, Ψ_L, g_s and k_L under water stress (Ψ_{soil}=-0.2), constant environmental conditions and variable guard cell osmotic adjustment (πg). A: πg augmented by 20%. B: πg diminished by 20%.

Figura 8. Simulaciones de embolia, Ψ_L, g_s y k_L bajo estrés hídrico (Ψ_{soil}=-0,2), circunstancias ambientales constantes y ajuste osmótico de la célula guardiana variable (πg). A: πg aumentado un 20%. B: πg disminuido un 20%.

Discussion

These measurements and the ideated mechanistic model, demonstrated that embolism and g_s are independent. Embolism rests on g_s only in addition to other plant and environmental variables; like xylem vulnerability, k_L, q´, g_b and Ψ_L. In this study g_s and k_L were tightly associated (R = 0.70). The model explained that daily embolism restraint was linked to variations of g_s in intimate relation with k_L. This tight relation between both conductances has already been widely observed in grapevine and trees (17, 21, 29, 39), evidencing that g_s responds to variations in k_L; and that both variables, in mutual interaction, control embolism in grapevines.

Apparently, k_L and g_s are related because, under drought, stomata operate allowing photosynthesis and preventing desiccation at the same time (7, 8). Consequently, g_s must respond to k_L, since changes in k_L influence plant and leaf water status (17). Therefore, the effect of g_s as prime embolism restraint attributed in grapevines and other species, could be related to the fact that both conductances are strongly coordinated (21, 29, 39). Regarding the generated model, it should be settled that the input variable k_L, is affected by intrinsic embolism, and involved in a feedback process.

The model measures embolism while k_L grows, (and it grows despite of the portion of hydraulic conductivity that embolism captures, probably given by the action of root aquaporins) (36). In fact, the model functions calculating embolism in a time t, from embolism in time t-1 (integrated in the input variable, k_L). This is correct in negative feedback mechanisms, as embolism's control shows to be (30). It might also be probable that this embolism that affects k_L is, partly, responsible for the stricter coupling between g_s and k_L. Nardini and Salleo (2000), explained that in many species embolism cannot be completely avoided and that it could constitute the signal that stomata need to start closing up. This can be reinterpreted as follows: stomata actually respond to a lower k_L caused by certain embolism formation, coupling itself to this changing k_L.

The obtained vulnerability curves were not different among treatments. Therefore, for the achieved water deficit, no xylem adaptation took place. It might be possible that differences among varieties were not evidenced because the stress levels achieved were not severe enough to generate these adaptation responses. It could also be possible that the experimental three months period was not long enough to let the xylem anatomically adapt to the stressful situation. Besides, the possibility of discriminating vulnerability differences turns to be quite hard, given that the phenomenon shows great intrinsic variability in grapevines and other species, (21, 22, 23, 35). For this study, variation coefficient for "lag" value was 0.55.

Of great importance is to highlight that in grapevines, embolism control does not require complete stomatal closure, meaning that photosynthesis is not completely deprived, and the assimilation cost is not as high as expected for other species.

In this experiment, under severe water stress (Ψ_{soil}=-0.2 MPa, and 50% embolism) g_s was significantly reduced but never achieved complete stomatal closure. In less stressful conditions, embolism is well controlled while stomata are still opened.

In 2011, Zufferey *et al.* (2011) found

that stomata closed up only after 90% of embolism was achieved. This means that the plant can keep on photosynthesizing and, at the same time, avoid catastrophic cavitation (cavitation levels at which the plant cannot recover and dyes). In this sense, it is one remarkable species that may require low amounts of water, and still produce quantity and quality of fruit, without the risk of suffering severe cavitation.

References

1. Alder, N.; Pockman, W.; Sperry, J. S.; Nuismer, S. 1997. Use of centrifugal force in the study of xylem cavitation. Journal of experimental botany. 48(3): 665-674.
2. Alsina, M. M.; Smart, D. R.; Bauerle, T.; De Herralde, F.; Biel, C.; Stockert, C.; Negron, C.; Save, R. 2011. Seasonal changes of whole root system conductance by a drought-tolerant grape root system. Journal of experimental botany. 62(1): 99-109.
3. Buckley, T.; Mott, K.; Farquhar, G. 2003. A hydromechanical and biochemical model of stomatal conductance. Plant, Cell & Environment. 26(10): 1767-1785.
4. Buckley, T. N. 2005. The control of stomata by water balance. New Phytologist. 168(2): 275-292.
5. Campbell, G. S.; Norman, J. M. 2012. An introduction to environmental biophysics: Springer Science & Business Media.
6. Chaves, M. M.; Maroco, J. P.; Pereira, J. S. 2003. Understanding plant responses to drought - From genes to the whole plant. Functional Plant Biology. 30(3): 239-264.
7. Chaves, M.; Oliveira, M. 2004. Mechanisms underlying plant resilience to water deficits: prospects for water-saving agriculture. Journal of experimental botany. 55(407): 2365-2384.
8. Chaves, M.; Zarrouk, O.; Francisco, R.; Costa, J.; Santos, T.; Regalado, A.; Rodrigues, M.; Lopes, C. 2010. Grapevine under deficit irrigation: hints from physiological and molecular data. Annals of Botany. 105(5): 661-676.
9. Chaves, M.; Costa, J.; Zarrouk, O.; Pinheiro, C.; Lopes, C.; Pereira, J. 2016. Controlling stomatal aperture in semi-arid regions-The dilemma of saving water or being cool? Plant Science. 251: 54-64.
10. Choat, B.; Drayton, W. M.; Brodersen, C.; Matthews, M. A.; Shackel, K. A.; Wada, H.; Mcelrone, A. J. 2010. Measurement of vulnerability to water stress-induced cavitation in grapevine: a comparison of four techniques applied to a long-vesseled species. Plant, Cell & Environment. 33(9): 1502-1512.
11. Cochard, H.; Coll, L.; Le Roux, X.; Améglio, T. 2002. Unraveling the effects of plant hydraulics on stomatal closure during water stress in walnut. Plant physiology. 128(1): 282-290.
12. Cochard, H.; Badel, E.; Herbette, S.; Delzon, S.; Choat, B.; Jansen, S. 2013. Methods for measuring plant vulnerability to cavitation: a critical review. Journal of experimental botany: p. ert193.
13. Dixon, H. H. 1914 Transpiration and the ascent of sap in plants: Macmillan and Company. 216 p.
14. Fernández, M. E.; Passera, C. B.; Cony, M. A. 2016. Sapling growth, water status and survival of two native shrubs from the Monte Desert, Mendoza, Argentina, under different preconditioning treatments. Revista de la Facultad de Ciencias Agrarias. Universidad Nacional de Cuyo. Mendoza. Argentina. 48(1): 33-47.
15. Franks, P. J.; Drake, P. L.; Froend, R. H. 2007. Anisohydric but isohydrodynamic: seasonally constant plant water potential gradient explained by a stomatal control mechanism incorporating variable plant hydraulic conductance. Plant, Cell & Environment. 30(1): 19-30.
16. Gerzon, E.; Biton, I.; Yaniv, Y.; Zemach, H.; Netzer, Y.; Schwartz, A.; Fait, A.; Ben-Ari, G. 2015. Grapevine anatomy as a possible determinant of isohydric or anisohydric behavior. American journal of enology and viticulture: p. ajev. 2015.14090.
17. Hsiao, T. C. 1990. Measurements of plant water status. In Irrigation of agricultural crops, B. A. Stewart and D. R. Nielsen, Editors. ASA, CSSA, SSSA: Madison. p. 243-279.

18. Hubbard, R. M.; Ryan, M.; Stiller, V.; Sperry, J. S. 2001. Stomatal conductance and photosynthesis vary linearly with plant hydraulic conductance in ponderosa pine. Plant, Cell & Environment. 24(1): 113-121.
19. Hugalde, I. P.; Vila, H. F. 2014. Isohydric or anisohydric behaviour in grapevine…, a never-ending controversy? RIA (Revista de Investigaciones Agrpecuarias). 40(1): 75-82.
20. Javot, H.; Maurel, C. 2002. The role of aquaporins in root water uptake. Annals of Botany. 90(3): 301-313.
21. Keller, M. 2015. The science of grapevines: anatomy and physiology: Academic Press. 522 p.
22. Lovisolo, C.; Perrone, I.; Hartung, W.; Schubert, A. 2008. An abscisic acid-related reduced transpiration promotes gradual embolism repair when grapevines are rehydrated after drought. New Phytologist. 180(3): 642-651.
23. Lovisolo, C.; Perrone, I.; Carra, A.; Ferrandino, A.; Flexas, J.; Medrano, H.; Schubert, A. 2010. Drought-induced changes in development and function of grapevine (Vitis spp.) organs and in their hydraulic and non-hydraulic interactions at the whole-plant level: A physiological and molecular update. Functional Plant Biology. 37(2): 98-116.
24. Lucero, C. C.; Di Filippo, M.; Vila, H.; Venier, M. 2017. Comparación de las respuestas al estrés hídrico y salino de los portainjertos de vid 1103P y 101-14Mgt, injertados con Cabernet Sauvignon. Revista de la Facultad de Ciencias Agrarias. Universidad Nacional de Cuyo. Mendoza. Argentina. 49(1): 33-43.
25. McDowell, N.; Pockman, W. T.; Allen, C. D.; Breshears, D. D.; Cobb, N.; Kolb, T.; Plaut, J.; Sperry, J.; West, A.; Williams, D. G. 2008. Mechanisms of plant survival and mortality during drought: why do some plants survive while others succumb to drought? New Phytologist. 178(4): 719-739.
26. Nardini, A.; Salleo, S. 2000. Limitation of stomatal conductance by hydraulic traits: sensing or preventing xylem cavitation? Trees-Structure and Function. 15(1): 14-24.
27. Phillips, N.; Ryan, M.; Bond, B.; McDowell, N.; Hinckley, T.; Cermak, J. 2003. Reliance on stored water increases with tree size in three species in the Pacific Northwest. Tree Physiology-Victoria. 23(4): 237-246.
28. Postaire, O.; Tournaire-Roux, C.; Grondin, A.; Boursiac, Y.; Morillon, R.; Schäffner, A. R.; Maurel, C. 2010. A PIP1 aquaporin contributes to hydrostatic pressure-induced water transport in both the root and rosette of Arabidopsis. Plant physiology. 152(3): 1418-1430.
29. Pou, A.; Medrano, H.; Flexas, J.; Tyerman, S. D. 2013. A putative role for TIP and PIP aquaporins in dynamics of leaf hydraulic and stomatal conductances in grapevine under water stress and re-watering. Plant, Cell and Environment. 36(4): 828-843.
30. Salleo, S.; Nardini, A.; Pitt, F.; Gullo, M. A. L. 2000. Xylem cavitation and hydraulic control of stomatal conductance in laurel (*Laurus nobilis* L.). Plant, Cell & Environment. 23(1): 71-79.
31. Sperry, J. S.; Saliendra, N.; Pockman, W.; Cochard, H.; Cruiziat, P.; Davis, S.; Ewers, F.; Tyree, M. 1996. New evidence for large negative xylem pressures and their measurement by the pressure chamber method. Plant, Cell & Environment. 19(4): 427-436.
32. Taiz, L.; Zeiger, E. 1998. Plant Physiology, 2nd. Ed. Sinauer. Sunderland. Massachussets. Available in: http://dx.doi.org/10.1071/PP9840361.
33. Tardieu, F.; Simonneau, T. 1998. Variability among species of stomatal control under fluctuating soil water status and evaporative demand: Modelling isohydric and anisohydric behaviours. Journal of Experimental Botany. 49(SPEC. ISS.): p. 419-432.
34. Tyree, M. T.; Sperry, J. S. 1989. Vulnerability of xylem to cavitation and embolism. Annual review of plant biology. 40(1): 19-36.
35. Tyree, M. T.; Zimmermann, M. H. 2002. Hydraulic architecture of whole plants and plant performance, in Xylem structure and the ascent of sap. Springer. p. 175-214.
36. Vandeleur, R. K.; Mayo, G.; Shelden, M. C.; Gilliham, M.; Kaiser, B. N.; Tyerman, S. D. 2009. The role of plasma membrane intrinsic protein aquaporins in water transport through roots: Diurnal and drought stress responses reveal different strategies between isohydric and anisohydric cultivars of grapevine. Plant Physiology. 149(1): 445-460.

37. Van den Honert, T. 1948. Water transport in plants as a catenary process. Discussions of the Faraday Society. 3: 146-153.
38. Zufferey, V.; Cochard, H.; Ameglio, T.; Spring, J.-L.; Viret, O. 2011. Diurnal cycles of embolism formation and repair in petioles of grapevine (*Vitis vinifera* cv. Chasselas). Journal of experimental botany: p. err081.
39. Zufferey, V.; Smart, D. 2012. Stomatal behaviour of irrigated *Vitis vinifera* cv. Syrah following partial root removal. Functional Plant Biology. 39(12): 1019-1027.

Acknowledgements

This work was supported by INTA EEA Mendoza, Argentina.
We thank Dr. Mark Matthews and Dr. Andrew McElrone (UC Davis, USA) for their critical reviews of the manuscript and valuable discussions.